Article | Received 11 August 2026; Revised 3 September; Accepted 5 September 2026; Published 24 September 2026
https://doi.org/10.55092/la20260011

Nanopore-based enzyme-linked immunosorbent assay for exosome detection

Xinyao Liu[1,2], Yakun Yi[1,*], Lei Liu[3] and Haichen Wu[1,2,*]

[1] Beijing National Laboratory for Molecular Sciences, Key Laboratory of Analytical Chemistry for Living Biosystems, Institute of Chemistry, Chinese Academy of Sciences, Beijing, China
[2] University of Chinese Academy of Sciences, Beijing, China
[3] College of Food and Bioengineering, Xihua University, Chengdu, China

* Correspondence authors; E-mails: yiyakun@iccas.ac.cn (Y.Y.); haichenwu@iccas.ac.cn (H.W.).

Highlights:

- An enzyme-assisted nanopore sensing platform is established for exosome analysis.
- Peptide substrates convert enzymatic reactions into distinguishable nanopore signals.
- The platform enables sensitive and quantitative exosome analysis down to 102 particles/mL.

Abstract: Exosomes contain abundant molecular information derived from parental cells and represent promising biomarkers for liquid biopsy. However, current exosome detection methods often suffer from complicated procedures, insufficient sensitivity, and limited applicability in complex biological samples. Herein, we developed a nanopore-based enzyme-linked immunosorbent assay (NELISA) for sensitive exosome analysis. This strategy employs exosomal surface antigens to construct alkaline phosphatase (ALP)-labelled sandwich immunocomplexes, followed by enzymatic conversion of the phosphorylated peptide probe FGpYD$_8$ (where "p" denotes phosphorylation modification). The substrate and product peptides generate distinct current signatures during translocation through a protein nanopore, enabling quantitative analysis through statistical evaluation of nanopore events. By rational selection of capture antibodies, the proposed method enables differential analysis of exosomes from distinct cellular origins and achieves a broad dynamic range of 10^2–10^9 particles/mL with a detection limit of 10^2 particles/mL for HeLa cell-derived exosomes, while maintaining reliable performance in complex biological matrices. This work provides a sensitive and versatile platform for exosome analysis and highlights its potential for exosome-based liquid biopsy applications.

Keywords: nanopore sensing; enzyme-linked immunosorbent assay; extracellular vesicles; exosome detection; biomarker analysis; liquid biopsy

Copyright©2026 by the authors. Published by ELSP. This work is licensed under Creative Commons Attribution 4.0 International License, which permits unrestricted use, distribution, and reproduction in any medium provided the original work is properly cited.

1. Introduction

Exosomes are a class of nanoscale extracellular vesicles (EVs) actively released by cells and characterized by a lipid bilayer membrane structure, with reported diameters typically ranging from 40 to 160 nm [1]. They are widely distributed in biological fluids, including blood, saliva, urine, and breast milk [2]. Exosomes carry abundant molecular information derived from their parental cells, including proteins, nucleic acids, and lipids [3]. The heterogeneity of these molecular cargos reflects the phenotypic characteristics, physiological states, and functional alterations of their cells of origin [1,3,4]. In particular, tumor-derived exosomes participate in intercellular communication and contribute to diverse biological processes, including tumor initiation and progression, immune regulation, metastasis, and therapeutic resistance [5]. The molecular signatures of tumor-associated exosomes can therefore provide valuable information for cancer diagnosis, prognosis evaluation, and disease monitoring [6]. Consequently, exosomes have emerged as promising biomarkers for liquid biopsy-based cancer detection [7–9].

Current strategies for exosome analysis largely rely on the recognition of surface proteins or molecular cargos. Flow cytometry is one of the most widely used approaches; however, its limited sensitivity toward small EVs may result in incomplete profiling of exosome populations and compromise analytical accuracy [10]. A variety of alternative methods, including colorimetric assays [11], fluorescence-based approaches [12,13], electrochemical sensing [14], and clustered regularly interspaced short palindromic repeats (CRISPR)-mediated strategies [15] have been developed for exosome detection. Despite these advances, achieving high sensitivity, accurate molecular profiling, and reliable performance in complex biological matrices remains challenging [16]. Therefore, the development of sensitive, specific, and facile analytical platforms is essential for advancing exosome-based liquid biopsy applications.

Nanopore sensing represents a powerful label-free single-molecule analytical technology that enables real-time molecular analysis through measurement of characteristic ionic current signatures generated by analyte translocation or interaction with nanopores [17,18]. Owing to its intrinsic single-molecule sensitivity, high throughput, and potential for miniaturization [19,20], nanopore sensing has been widely applied in ion detection [21,22], molecular detection [23,24], biomolecular analysis [25,26], single-molecule chemistry [27–29], disease biomarker detection [30–32], DNA sequencing [33–35], amino acids discrimination [36] and protein sequencing based on full-length chain [37–41] and enzyme-assisting [42–44]. In our previous studies, we established an enzyme-assisted nanopore sensing platform that converts conventional enzymatic recognition events into electrical signals using enzyme-responsive peptide probes, enabling sensitive quantitative detection of various biomarkers, including antigens, antibodies, and nucleic acids [45,46]. Here, we extend this strategy to exosome analysis by developing a nanopore-based enzyme-linked immunosorbent assay (NELISA). This platform utilizes exosomal surface antigen recognition to construct alkaline phosphatase (ALP)-labeled sandwich immunocomplexes, in which ALP-mediated conversion of the phosphorylated peptide probe $FGpYD_8$ generates distinguishable nanopore current signatures. The resulting NELISA enables quantitative detection of HeLa cell-derived extracellular vesicles with a broad dynamic range of 10^2–10^9 particles/mL and a detection limit of 10^2 particles/mL. Furthermore, by exploiting heterogeneous surface antigen expression patterns, this approach provides a strategy for differential

analysis of extracellular vesicles derived from distinct cellular origins, highlighting its potential for exosome-based liquid biopsy applications.

2. Methods

2.1. Materials and characterization

1,2-Diphytanoyl-*sn*-glycero-3-phosphochline (DPhPc) was purchased from Avanti Polar Lipids (Alabaster, AL). $FGpYD_8$ were purchased from QYAOBIO (ChinaPeptides Co., Ltd.) and purified by HPLC. All antibodies were purchased from Bioss Biotechnology Co., Ltd (Beijing). All antigen standard samples and alkaline phosphatase labelled streptavidin were purchased from Sangon Biotechnology (Shanghai). Fetal bovine serum (FBS) was purchased from Gibco, Thermo Fisher Scientific (Waltham, MA, USA). The peptide samples were dissolved in deionized water (Millipore, MA) and stored at −20 °C. Wild type α-hemolysin-D8H6 (αHL) proteins were produced as described previously [18].

2.2. Buffer preparation

Coating buffer for ELISA. 0.7500 g of Na_2CO_3 (99.9%, Sigma-Aldrich), 1.4600 g of $NaHCO_3$ (99.9%, Sigma-Aldrich) were dissolved in 450.0 mL of deionized water (Millipore, MA). 2.0 M NaOH was used to adjust the pH to 9.6. The solution was diluted with deionized water to 500.0 mL. The final buffer solution consists of 50.0 mM carbonate at pH 9.6.

Blocking buffer for ELISA. 2.0000 g of BSA (99.0%, Sigma-Aldarich) was dissolved with coating buffer and diluted to 100.0 mL.

Washing buffer for ELISA. 500.0 μL of Tween-20, 2.9000 g of $Na_2HPO_4 \cdot 12H_2O$, 0.2000 g of KH_2PO_4, 8.0000 g of NaCl were dissolved in 950.0 mL of deionized water. 2.0 M NaOH was used to adjust the pH to 7.4. The solution was diluted with deionized water to 1.0 L. The final buffer solution consists of 0.05% Tween-20, 150.0 mM NaCl, 20.0 mM PBS at pH 7.4.

Antibody dilution buffer for ELISA. 0.6050 g of Trizma (99.9%, Sigma-Aldarich), 0.8750 g of NaCl and 1.0000 g of BSA were dissolved in 95 mL of deionized water. 2.0 M HCl was used adjust the pH to 7.4. The solution was diluted with deionized water to 100.0 mL. The final buffer solution consists of 1.0 % BSA, 150 mM NaCl, 50 mM Tris at pH 7.4.

Sample dilution buffer for ELISA. 0.1000 g BSA was dissolved with washing buffer to 100.0 mL.

Assay buffer. 0.4383 g of NaCl (99.9%, Sigma-Aldrich), 0.0969 g Trizma (99.9%, Sigma-Aldrich), 0.0081 g of $MgCl_2 \cdot 6H_2O$ (99.9%, Sigma-Aldrich) were dissolved in 40.0 mL of deionized water (Millipore, MA). 2.0 M HCl was used to adjust the pH to 9.0. The solution was diluted with deionized water to 50.0 mL. The final buffer solution consists of 150.0 mM NaCl, 20.0 mM Tris, 2.0 mM $MgCl_2$ at pH 9.0.

2.3. Methods for exosomes detection

Preparation of capture antibody-coated plates. The antibody was diluted to 2.0 μg/mL with coating buffer. 100.0 μL of the solution was added to each well of a 96-well microassay plate. The plate was incubated at 4.0 ℃ overnight covered with plastic film sheets. After incubation, the plate was washed with washing buffer three times and blocked with blocking buffer at 37 ℃ for 4 h. And

then, the plate was washed with washing buffer for three times and covered with plastic film sheets, stored at 4.0 ℃ or used for next step.

Exosomes-capture antibody interactions. 100.0 μL Exosomes solutions or sample solutions were added to different wells of the plate and incubated at 37 ℃ for 90 min. After incubation, the plate was washed with washing buffer for three times and then used for next step.

Preparation of alkaline phosphatase-labelled anti-CD63 detection complex. ALP-labeled streptavidin was diluted to 100.0 μg/mL and biotinylated anti-CD63 antibody was diluted to 50.0 μg/mL with dilution buffer. The two solutions were 1:1 (v/v) mixed and incubated at 37 ℃ for 60 min to form the ALP-labelled anti-CD63 detection complex through biotin–streptavidin interaction. The resulting complex was diluted 25-fold before use in the subsequent detection step.

Antigen-detection antibody interactions. 100.0 μL ALP-labelled anti-CD63 were added to each well of the plate and incubated at 37 ℃ for 60 min. After incubation, the plate was washed with washing buffer for three times and then used for next steps.

Enzymatic reaction. The peptide $FGpYD_8$ were diluted to 2.5 μM with assay buffers. 100.0 μL of the solution was added to each well of the plate and incubated at 37 ℃ for 60 min. The incubation was terminated by transferring the solutions into tubes, which were then stored at −20 °C for single-channel recording experiments.

2.4. Single-channel current recordings

1,2-Diphytanoyl-*sn*-glycero-3-phosphocholine was used to form a synthetic lipid bilayer across an aperture 100-150 μm in diameter in a 25-μm-thick polytetrafluoroethylene film (Goodfellow, Malvern, PA) that divided a chamber into two compartments, cis and trans. Both compartments contained 1.0 mL of buffer solution. 40.0 μL enzymatic reaction product solution and 5.0 μL CB[7] (5.0 mM) were added to the cis compartment, which was connected to ground. The trans compartment was connected to the head-stage of the amplifier. All experiments were carried out in 1.0 M KCl, 10.0 mM PBS, pH 5.0 in *cis*, 3.6 M KCl, 10.0 mM PBS, pH 5.0 in *trans*, at 23 ± 2 °C. Ionic currents were measured using Ag/AgCl electrodes with a patch-clamp amplifier (Axopatch 200B; Axon instruments, Foster City, CA), filtered with a low-pass Bessel filter with a corner frequency of 10 kHz and then digitized with a Digidata 1550B A/D converter (Axon Instruments) at a sampling frequency of 100 kHz. The potential was held at +200 mV unless otherwise stated.

2.5. Data analysis

Current traces were analyzed with Clampfit 11.7 software (Axon Instruments). Events were identified based on characteristic current blockade amplitudes (I/I_0) of peptide translocation. The event frequency was calculated by dividing the number of characteristic events by the recording duration. For each sample, current traces were recorded for at least 10 min, and the same event identification criteria were applied for all measurements. OriginPro 2024 (Microcal, Northampton, MA) and Clampfit 11.7 were used for histogram construction, curve fitting and graph presentation. Adobe Illustrator 2023 was used for making figures.

3. Results

Principle of the NELISA for exosome detection. The NELISA-based exosome detection strategy relies on the construction of a sandwich immunocomplex on a solid-phase interface. As illustrated in Figure 1, capture antibodies pre-coated on the microplate recognize surface antigens on target exosomes. Subsequently, an ALP-labelled detection antibody is introduced to form a sandwich immunocomplex. Following immunocomplex formation, the phosphorylated peptide probe $FGpYD_8$ is added as an enzymatic reporter. The ALP associated with the immunocomplex catalyzes the dephosphorylation of $FGpYD_8$, converting it into $FGYD_8$. After incubation, the reaction products are collected and introduced into an α-hemolysin (αHL) nanopore sensing system in the presence of cucurbit [7] uril (CB [7]). Owing to their distinct interactions with the nanopore, the substrate peptide $FGpYD_8$ and the dephosphorylated product $FGYD_8$ generate distinguishable ionic current signatures, enabling single-molecule-level readout of the enzymatic conversion (Figure 2a). Because the amount of ALP captured on the microplate depends on the abundance of antigen-positive exosomes, higher concentrations of target exosomes result in increased enzymatic conversion of $FGpYD_8$ during a fixed reaction period. Consequently, the residual $FGpYD_8$ event frequency decreases with increasing exosome concentration, providing a quantitative readout for exosome analysis.

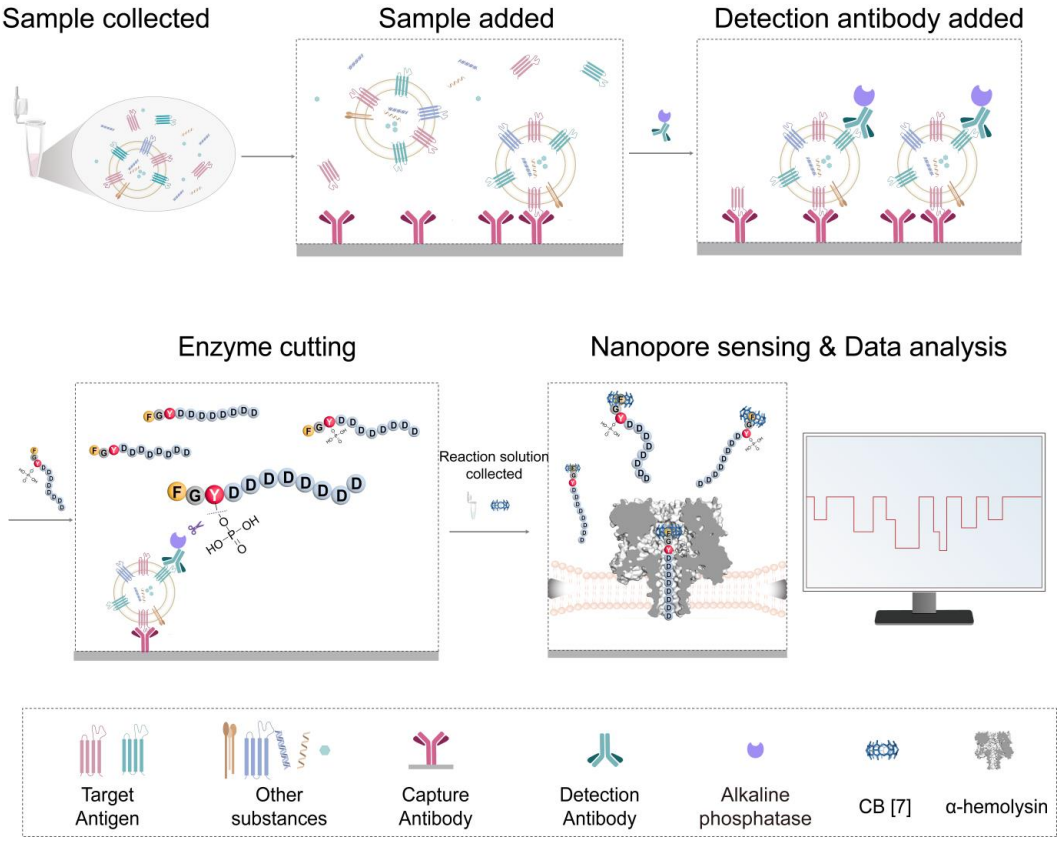

Figure 1. Schematic diagram of the NELISA for exosomes detection. samples containing exosomes were obtained through the exosomes isolation from cell culture medium using isolation reagent. these samples were then added to plate wells precoated with a capture antibody. the enzyme-labelled detection antibody was subsequently added to form a sandwich structure. after washing, peptide probe was introduced to the wells to interact with the enzyme. finally, the sample solution was collected for nanopore translocation measurements.

We first selected CD63, a commonly used exosomal surface marker, as the target antigen for both capture and detection antibodies, and demonstrated the feasibility of the NELISA strategy using HeLa cell-derived exosomes (Figure S1). In high exosome concentration samples, the $FGpYD_8$ event frequency decreased to 175 min^{-1}, representing a substantial reduction compared with 383 min^{-1} obtained in the PBS control (Figure 2b). This decrease resulted from ALP-mediated consumption of $FGpYD_8$ during the enzymatic reaction, confirming the feasibility of converting exosome recognition events into nanopore-readable signals. Subsequently, the concentration of the peptide substrate was optimized (Figure S2), and 2.5 μM $FGpYD_8$ was selected as the optimal substrate concentration for subsequent NELISA measurements.

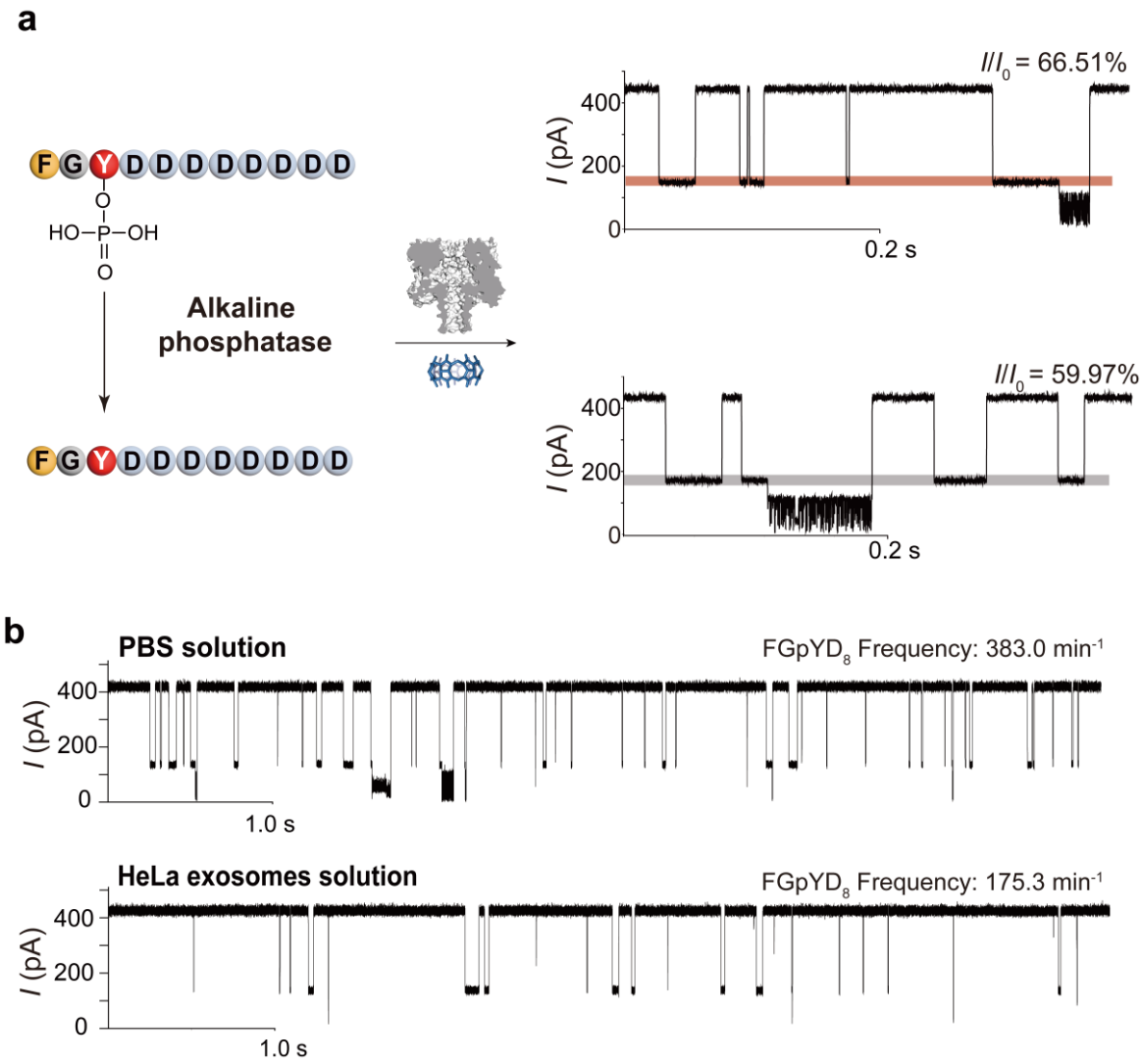

Figure 2. Current signal alterations during exosomes detection. **(a)** Enzymatic cleavage of $FGpYD_8$ by alkaline phosphatase and the corresponding translocation current signal changes; **(b)** Current traces of NELISA for different samples (top: PBS solution, bottom: HeLa exosome solution). all data were acquired in a buffer comprising 3.6 M KCl, 10.0 mM PBS and pH 5.0 in *trans* compartment and 1.0 M KCl, 10.0 mM PBS and pH 5.0 in *cis* compartment, with the transmembrane potential held at +200 mV. event frequency represents the number of characteristic peptide translocation events detected per minute.

Differential analysis of exosomes derived from different cell types. Exosomes derived from different cell types exhibit heterogeneous surface antigen compositions and expression levels, providing a potential strategy for differential analysis of exosomes from distinct cellular origins. To explore this possibility, exosomes derived from HEK293 and HeLa cells were cultured separately and isolated under identical conditions (Figure S3). Antibodies against CD63, CEA, EGFR, and EpCAM were individually employed as capture antibodies, while an ALP-labelled anti-CD63 antibody was used as the detection antibody. NELISA was subsequently applied to analyze HEK293- and HeLa-derived exosomes at a concentration of 10^8 particles/mL (Figure S4). To compare the influence of different capture antibodies on exosome analysis, the $FGpYD_8$ event frequency obtained from HEK293-derived exosomes using each capture antibody was normalized to 1.0, and the corresponding values for HeLa-derived exosomes were calculated accordingly (Figure 3). Among the tested capture antibodies, the EpCAM-based assay produced a substantially lower $FGpYD_8$ frequency for HeLa-derived exosomes compared with HEK293-derived exosomes, whereas assays using the other capture antibodies showed comparable responses between the two exosome sources. These results demonstrate that heterogeneous surface antigen expression patterns of exosomes can be exploited for differential analysis of vesicles derived from distinct cellular origins. With appropriate selection and combination of surface biomarkers, the NELISA platform may provide a promising approach for multiplexed profiling and characterization of exosomal surface signatures.

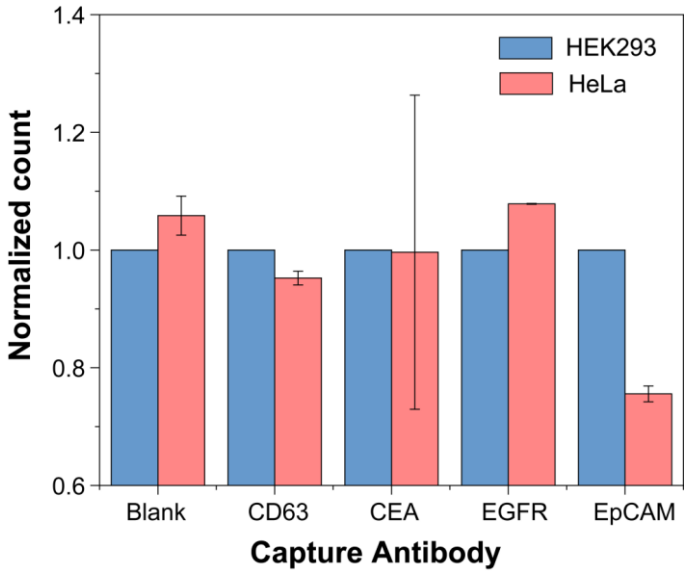

Figure 3. Selection of capture antibody. normalized NELISA measurement results of HEK293- and HeLa-derived exosomes with different capture antibodies all data were acquired in a buffer comprising 3.6 M KCl, 10.0 mM PBS and pH 5.0 in *trans* compartment and 1.0 M KCl, 10.0 mM PBS and pH 5.0 in *cis* compartment, with the transmembrane potential held at +200 mV. data are presented as mean ± SD (n = 3) from three independent experiments.

Analytical performance of NELISA for exosome detection. Under the optimized conditions established above, a series of gradient-diluted HeLa-derived exosome samples were analyzed using the NELISA platform for quantitative evaluation. The NELISA assay exhibited a broad dynamic response range from 10^2 to 10^9 particles/mL, with a limit of detection (LOD) of 10^2 particles/mL for HeLa-derived

exosomes (Figure 4a). Compared with previously reported exosome detection methods, the NELISA platform demonstrates a broad quantitative range and high analytical sensitivity (Table S1). Furthermore, the specificity of the NELISA was evaluated using several common protein tumor biomarkers as potential interfering substances. As shown in Figure 4b, only exosome samples induced a substantial change in $FGpYD_8$ event frequency, whereas free protein antigens produced responses comparable to the blank control. These results indicate that soluble protein antigens potentially present in biological samples have minimal interference with the NELISA measurement, highlighting the high specificity of the immunorecognition-based strategy. Overall, these results indicate the NELISA enables sensitive and quantitative exosome analysis with a broad dynamic range, providing a promising platform for exosome-based biomarker analysis.

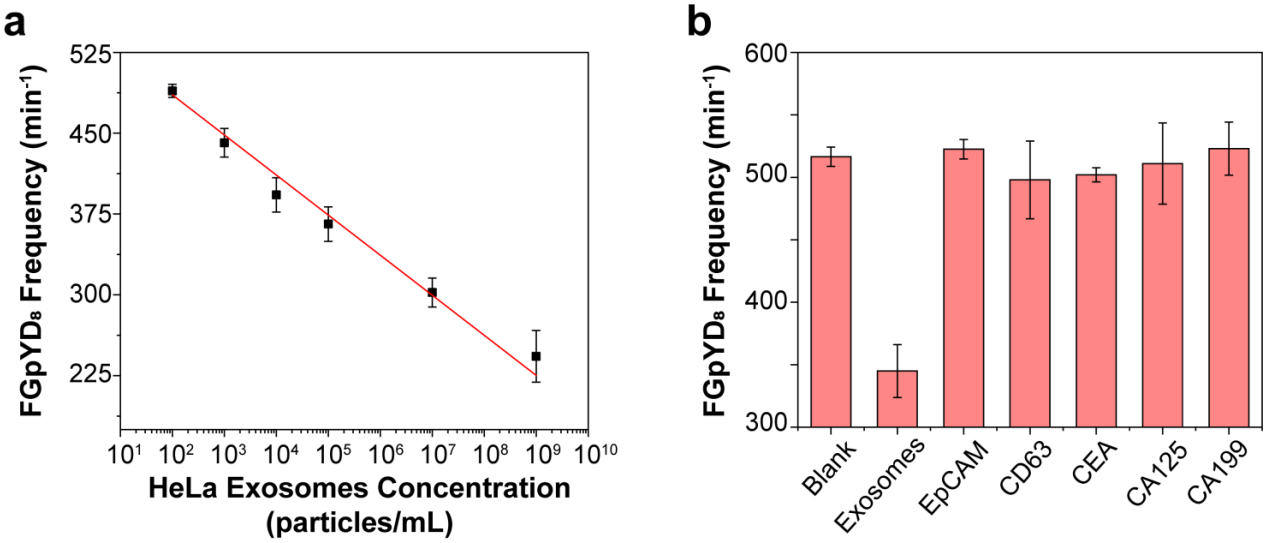

Figure 4. Performance of exosomes detection. **(a)** Correlation of event frequency with the concentration of HeLa-derived exosomes in the range of 10^2–10^9 particles/mL various concentrations of HeLa-derived exosomes (10^2, 10^3, 10^4, 10^5, 10^7, 10^9 particles/mL) were detected with alkaline phosphatase in ELISA step. Then, the samples and CB [7] were added to the nanopore system to achieve final concentrations of 100.0 nM probe and 25.0 μM CB [7] in the detection system. the linear equation is $y = -37.18 \lg x + 559.94$, $R^2 = 0.989$. limit of detection is 10^2 particles/mL; **(b)** Specificity of NELISA for exosomes detection. 10^9 particles/mL of HeLa-derived exosomes and different types of protein antigens (1.0 μg/mL EpCAM, 1.0 μg/mL CD63, 190 ng/mL CEA, 400 U/mL CA19-9 and 500 U/mL CA125) are used in the ELISA step. Then, samples and CB [7] were added to the nanopore system to achieve final concentrations of 100.0 nM probe and 25.0 μM CB [7] in the detection system. all data were acquired in a buffer comprising 3.6 M KCl, 10.0 mM PBS and pH 5.0 in *trans* compartment and 1.0 M KCl, 10.0 mM PBS and pH 5.0 in *cis* compartment, with the transmembrane potential held at +200 mV. Data are presented as mean ± SD (n = 3) from three independent experiments.

Feasibility of NELISA for exosome detection in complex biological matrices. To further evaluate the robustness of the proposed method in complex biological environments, exosome spike-in experiments were performed in 10% FBS samples (FBS:PBS = 1:9, v/v). The 10% FBS model matrix contains abundant proteins and other biomolecular components that may interfere with immunorecognition and nanopore-based signal readout. Despite the presence of these potential interfering substances, the

NELISA platform maintained a quantitative response range of 10^2–10^9 particles/mL and achieved the same limit of detection (10^2 particles/mL) as that obtained in PBS samples (Figure 5). These results demonstrate the excellent matrix tolerance of the NELISA platform and indicate that the combination of specific antibody recognition and nanopore-based molecular readout enables reliable exosome analysis under biologically relevant conditions. This capability highlights the potential of NELISA as a sensitive platform for extracellular vesicle analysis in real biological samples containing a large amount of interfering substances.

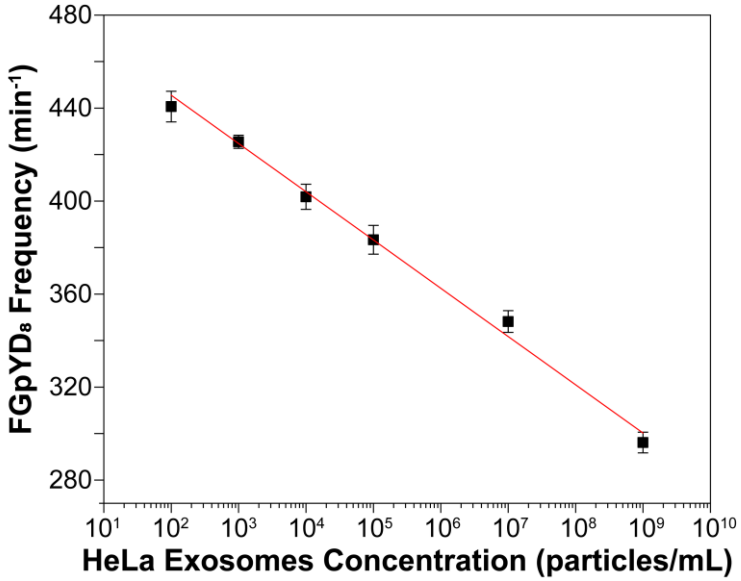

Figure 5. Detection results of HeLa-derived exosomes in 10% FBS spiked samples. The working curves of HeLa-derived exosomes obtained from 10% FBS spiked samples. Linear equation is $y = -20.75 \lg x + 487.03$, $R^2 = 0.995$. All data were acquired in a buffer comprising 3.6 M KCl, 10.0 mM PBS and pH 5.0 in *trans* compartment and 1.0 M KCl, 10.0 mM PBS and pH 5.0 in *cis* compartment, with the transmembrane potential held at +200 mV. Data are presented as mean ± SD (n = 3) from three independent experiments.

4. Conclusion

Overall, this study establishes a NELISA platform for sensitive and quantitative exosome analysis. By integrating antibody-mediated molecular recognition, enzyme-amplified peptide conversion, and nanopore single-molecule readout, NELISA overcomes the limitations of conventional exosome detection methods in terms of sensitivity and signal transduction. The proposed platform achieves a broad quantitative range of 10^2–10^9 particles/mL with a detection limit of 10^2 particles/mL, while maintaining reliable performance in the presence of soluble antigens and complex biological matrices.

Despite these advances, the application of this method to exosome-based liquid biopsy still faces several challenges in practical use, including the heterogeneity of exosomal populations, the lack of universally specific surface markers, and the complexity associated with exosome isolation from biological samples. Future integration of multiple surface biomarkers, standardized exosome enrichment strategies, and automated sample processing may further improve the accuracy and robustness of NELISA for exosome profiling. In addition, coupling the nanopore sensing platform with miniaturized

instrumentation could facilitate the development of portable and high-throughput analytical systems. Collectively, this work provides a versatile strategy for translating exosome-associated molecular information into electrical signals and establishes a foundation for next-generation extracellular vesicle analysis in biomedical research and liquid biopsy applications.

Data availability statement

A supplementary file is provided with this article, containing additional experimental methods, nanoparticle tracking analysis (NTA) characterization of cell-derived exosomes, optimization of the peptide probe concentration, screening of capture antibodies, and a comparison of the analytical performance with previously reported exosome detection methods.

Declaration of generative AI and AI-assisted technologies

During the preparation of this manuscript, the authors used generative AI tools only to improve language and readability. Specifically, the authors used ChatGPT for language polishing only in limited sections of the manuscript. The intellectual content of the manuscript (including ideas, analysis, and conclusions) is original work, and the manuscript complies with academic integrity and publication ethics standards.

Acknowledgments

Funding: This work was funded by the National Natural Science Foundation of China (No. 22374151 to L.L.; No. 22025407, 22427807 to H.W.), the Strategic Priority Research Program of the Chinese Academy of Sciences (Grant No. XDB0960200) and Institute of Chemistry, Chinese Academy of Sciences. The funders had no role in study design, data collection and analysis, decision to publish or preparation of the manuscript.

Authors' contribution

Conceptualization, Y.Y., L.L. and H.W.; methodology, X.L. and Y.Y.; validation, X.L.; formal analysis, X.L.; data curation, X.L. and Y.Y.; writing—original draft preparation, X.L. and Y.Y.; writing—review and editing, L.L. and H.W.; visualization, X.L. and Y.Y.; supervision, L.L. and H.W.; project administration, L.L. and H.W.; funding acquisition, L.L. and H.W. All authors have read and agreed to the published version of the manuscript.

Conflicts of interest

Haichen Wu holds the position of Editorial Board Member for *Life Analysis* and has not peer reviewed or made any editorial decisions for this paper.

References

[1] Kalluri R, LeBleu VS. The biology, function, and biomedical applications of exosomes. *Science* 2020, 367(6478):eaau6977.

[2] Vlassov AV, Magdaleno S, Setterquist R, Conrad R. Exosomes: current knowledge of their composition, biological functions, and diagnostic and therapeutic potentials. *Biochim. Biophys. Acta Gen. Subj.* 2012, 1820(7):940–948.
[3] Van Niel G, D'Angelo G, Raposo G. Shedding light on the cell biology of extracellular vesicles. *Nat. Rev. Mol. Cell Biol.* 2018, 19(4):213–228.
[4] Kowal J, Arras G, Colombo M, Jouve M, Morath JP, *et al.* Proteomic comparison defines novel markers to characterize heterogeneous populations of extracellular vesicle subtypes. *Proc. Natl. Acad. Sci. U. S. A.* 2016, 113(8):E968–E977.
[5] Maia J, Caja S, Strano Moraes MC, Couto N, Costa-Silva B. Exosome-based cell-cell communication in the tumor microenvironment. *Front. Cell Dev. Biol.* 2018, 6:18.
[6] Hoshino A, Costa-Silva B, Shen TL, Rodrigues G, Hashimoto A, *et al.* Tumour exosome integrins determine organotropic metastasis. *Nature* 2015, 527(7578):329–335.
[7] Shao H, Chung J, Issadore D. Diagnostic technologies for circulating tumour cells and exosomes. *Biosci. Rep.* 2016, 36(1):e00292.
[8] Li L, Zhang L, Montgomery KC, Jiang L, Lyon CJ, *et al.* Advanced technologies for molecular diagnosis of cancer: state of pre-clinical tumor-derived exosome liquid biopsies. *Mater. Today Bio.* 2023, 18:100538.
[9] Zhou B, Xu K, Zheng X, Chen T, Wang J, *et al.* Application of exosomes as liquid biopsy in clinical diagnosis. *Signal Transduct. Target. Ther.* 2020, 5(1):144.
[10] Wang Z, Zhang Z, Zhang Y, Xu X, Shen T, *et al.* MXenes-Au NPs modified electrochemical biosensor for multiple exosome surface proteins analysis. *Talanta* 2023, 265:124848.
[11] He F, Liu H, Guo X, Yin B, Ye B. Direct exosome quantification via bivalent-cholesterol-labeled DNA anchor for signal amplification. *Anal. Chem.* 2017, 89(23):12968–12975.
[12] Wan S, Zhang L, Wang S, Liu Y, Wu C, *et al.* Molecular recognition-based DNA nanoassemblies on the surfaces of nanosized exosomes. *J. Am. Chem. Soc.* 2017, 139(15):5289–5292.
[13] He D, Ho SL, Chan H, Wang H, Hai L, *et al.* Molecular-recognition-based DNA nanodevices for enhancing the direct visualization and quantification of single vesicles of tumor exosomes in plasma microsamples. *Anal. Chem.* 2019, 91(4):2768–2775.
[14] Huang R, He L, Xia Y, Xu H, Liu C, *et al.* A sensitive aptasensor based on a hemin/G-quadruplex-assisted signal amplification strategy for electrochemical detection of gastric cancer exosomes. *Small* 2019, 15(19):e1900735.
[15] Zhao X, Zeng L, Mei Q, Luo Y. Allosteric probe-initiated wash-free method for sensitive extracellular vesicle detection through dual cycle-assisted CRISPR-Cas12a. *ACS Sens.* 2020, 5(7):2239–2246.
[16] Li S, Ma Q. Electrochemical nano-sensing interface for exosomes analysis and cancer diagnosis. *Biosens. Bioelectron.* 2022, 214:114554.
[17] Bayley H, Cremer PS. Stochastic sensors inspired by biology. *Nature* 2001, 413(6852):226–230.
[18] Ying Y, Hu Z, Zhang S, Qing Y, Fragasso A, *et al.* Nanopore-based technologies beyond DNA sequencing. *Nat. Nanotechnol.* 2022, 17(11):1136–1146.
[19] Siwy ZS, Howorka S. Engineered voltage-responsive nanopores. *Chem. Soc. Rev.* 2010, 39(3):1115–1132.
[20] Wu Y, Gooding JJ. The application of single molecule nanopore sensing for quantitative analysis. *Chem. Soc. Rev.* 2022, 51(10):3862–3885.

[21] Wen S, Zeng T, Liu L, Zhao K, Zhao Y, *et al.* Highly sensitive and selective DNA-based detection of mercury (II) with α-hemolysin nanopore. *J. Am. Chem. Soc.* 2011, 133(45):18312–18317.
[22] Braha O, Walker B, Cheley S, Kasianowicz JJ, Song L, *et al.* Designed protein pores as components for biosensors. *Chem. Biol.* 1997, 4(7):497–505.
[23] Gu LQ, Braha O, Conlan S, Cheley S, Bayley H. Stochastic sensing of organic analytes by a pore-forming protein containing a molecular adapter. *Nature* 1999, 398(6729):686–690.
[24] Jia W, Hu C, Wang Y, Gu Y, Qian G, *et al.* Programmable nano-reactors for stochastic sensing. *Nat. Commun.* 2021, 12:5811.
[25] Galenkamp NS, Biesemans A, Maglia G. Directional conformer exchange in dihydrofolate reductase revealed by single-molecule nanopore recordings. *Nat. Chem.* 2020, 12(5):481–488.
[26] Jiang J, Li M, Wu X, Ying Y, Han H, *et al.* Protein nanopore reveals the renin–angiotensin system crosstalk with single-amino-acid resolution. *Nat. Chem.* 2023, 15(4):578–586.
[27] Lu S, Li WW, Rotem D, Mikhailova E, Bayley H. A primary hydrogen-deuterium isotope effect observed at the single-molecule level. *Nat. Chem.* 2010, 2(11):921–928.
[28] Qing Y, Ionescu SA, Pulcu GS, Bayley H. Directional control of a processive molecular hopper. *Science* 2018, 361(6405):908–912.
[29] Hammerstein AF, Shin SH, Bayley H. Single-molecule kinetics of two-step divalent cation chelation. *Angew. Chem. Int. Ed.* 2010, 49(30):5085–5090.
[30] Chen X, Zhang Y, Mohammadi Roozbahani G, Guan X. Salt-mediated nanopore detection of ADAM-17. *ACS Appl. Bio Mater.* 2019, 2(1):504–509.
[31] Wang Y, Zheng D, Tan Q, Wang MX, Gu LQ. Nanopore-based detection of circulating microRNAs in lung cancer patients. *Nat. Nanotechnol.* 2011, 6(10):668–674.
[32] Zhang J, Liu X, Hu Z, Ying Y, Long Y. Intelligent identification of multi-level nanopore signatures for accurate detection of cancer biomarkers. *Chem. Commun.* 2017, 53(73):10176–10179.
[33] Clarke J, Wu H, Jayasinghe L, Patel A, Reid S, *et al.* Continuous base identification for single-molecule nanopore DNA sequencing. *Nat. Nanotechnol.* 2009, 4(4):265–270.
[34] Manrao EA, Derrington IM, Laszlo AH, Langford KW, Hopper MK, *et al.* Reading DNA at single-nucleotide resolution with a mutant MspA nanopore and phi29 DNA polymerase. *Nat. Biotechnol.* 2012, 30(4):349–353.
[35] Flusberg BA, Webster DR, Lee JH, Travers KJ, Olivares EC, *et al.* Direct detection of DNA methylation during single-molecule, real-time sequencing. *Nat. Methods* 2010, 7(6):461–465.
[36] Ouldali H, Sarthak K, Ensslen T, Piguet F, Manivet P, *et al.* Electrical recognition of the twenty proteinogenic amino acids using an aerolysin nanopore. *Nat. Biotechnol.* 2020, 38(2):176–181.
[37] Brinkerhoff H, Kang AS, Liu J, Aksimentiev A, Dekker C. Multiple rereads of single proteins at single–amino acid resolution using nanopores. *Science* 2021, 374(6574):1509–1513.
[38] Motone K, Kontogiorgos-Heintz D, Wee J, Kurihara K, Yang S, *et al.* Multi-pass, single-molecule nanopore reading of long protein strands. *Nature* 2024, 633(8030):662–669.
[39] Yan S, Zhang J, Wang Y, Guo W, Zhang S, *et al.* Single molecule ratcheting motion of peptides in a *Mycobacterium smegmatis* porin A (MspA) nanopore. *Nano Lett.* 2021, 21(15):6703–6710.
[40] Chen Z, Wang Z, Xu Y, Zhang X, Tian B, *et al.* Controlled movement of ssDNA conjugated peptide through *Mycobacterium smegmatis* porin A (MspA) nanopore by a helicase motor for peptide sequencing application. *Chem. Sci.* 2021, 12(47):15750–15756.

[41] Yu L, Kang X, Li F, Mehrafrooz B, Makhamreh A, *et al.* Unidirectional single-file transport of full-length proteins through a nanopore. *Nat. Biotechnol.* 2023, 41(8):1130–1139.

[42] Zhang Y, Yi Y, Li Z, Zhou K, Liu L, *et al.* Peptide sequencing based on host–guest interaction-assisted nanopore sensing. *Nat. Methods* 2024, 21(1):102–109.

[43] Zhang M, Tang C, Wang Z, Chen S, Zhang D, *et al.* Real-time detection of 20 amino acids and discrimination of pathologically relevant peptides with functionalized nanopore. *Nat. Methods* 2024, 21(4):609–618.

[44] Wang K, Zhang S, Zhou X, Yang X, Li X, *et al.* Unambiguous discrimination of all 20 proteinogenic amino acids and their modifications by nanopore. *Nat. Methods* 2024, 21(1):92–101.

[45] Yi Y, Song P, Li Z, Ju J, Sun G, *et al.* Nanopore-based enzyme-linked immunosorbent assay for cancer biomarker detection. *Nat. Nanotechnol.* 2025, 20(8):1079–1086.

[46] Huang X, Yi Y, Zhou K, Liu L, Wu H. Enzyme-assisted nanopore sensor for sensitive and multiplexed detection of microRNAs. *J. Nanobiotechnol.* 2025, 24(1):88.